Quaternary Research (2022), **110**, 1–12
doi:10.1017/qua.2022.31

Research Article

Holocene climate background for lake evolution in the Badain Jaran Desert of northwestern China revealed by proxies from calcareous root tubes

Zhuolun Li[a,b*], Xiang Li[a], Shipei Dong[a] and Youhong Gao[a]

[a]College of Earth and Environmental Sciences, Center for Glacier and Desert Research, Lanzhou University, 730030 Lanzhou, China and [b]Key Laboratory of Quaternary Chronology and Hydro-Environmental Evolution, China Geological Survey, 050061 Shijiazhuang, China

Abstract

It has been unclear whether Holocene lake evolution in the Badain Jaran Desert of northwestern China, an area in which lakes are mainly recharged by groundwater, responded to climate change. In this study, we analyzed the Mg/Ca ratio and phytolith assemblages from 10 Holocene calcareous root tube samples from the desert to reconstruct changes in effective moisture and mean annual precipitation (MAP) at the millennial scale during the Holocene and to explore the factors affecting lake evolution. Our results revealed that the effective moisture at 7000–5000 cal yr BP was higher than that of 5000–2000 cal yr BP. Similarly, the MAP was higher at 7000–5000 cal yr BP (175 ± 37 to 205 ± 37 mm) than at 5000–2000 cal yr BP (145 ± 37 to 165 ± 39 mm). The expansion of the lakes during the Early Holocene would have resulted from the input of groundwater from the meltwater in the recharge area. High lake levels in the Middle Holocene corresponded to increased monsoonal precipitation and groundwater recharge. The gradual decline of lake levels in the Late Holocene indicated a relatively arid climate with decreased monsoonal precipitation and groundwater recharge.

Keywords: Holocene, Sand sea, Lake evolution, Climate change, Pedogenic carbonate, Phytolith, Northwestern China

(Received 27 November 2021; accepted 24 May 2022)

INTRODUCTION

Lakes can be viewed as connections and points of interaction between subsystems of Earth and thus serve as important archives for global environmental changes (Goldsmith et al., 2017; Tierney et al., 2020). Paleoenvironmental changes at different timescales can be reconstructed based on proxy records from lake sediments and landforms (Zhang et al., 2004; Melnick et al., 2012; Wang et al., 2012, 2019). However, the relationship between lake evolution and the hydrological cycle in arid and semiarid regions is complex (Yang and Scuderi, 2010; Garcin et al., 2012; Shen, 2013; Wang et al., 2016). Such changes are influenced by both climatic factors, including precipitation and evaporation (Yang et al., 2010; Jin et al., 2015), and non-climatic factors, such as neotectonics (Wang and Ji, 1995), river diversion (Jin et al., 2015), and glacial meltwater input (Fan et al., 2019). In some areas, non-climatic impact factors play a more important role in lake evolution than climatic factors (Hartmann and Wünnemann, 2009; Yang and Scuderi, 2010). Therefore, determining the driving factors for lake evolution in arid and semiarid regions is essential for the accurate assessment of paleoenvironmental changes. Moreover, this will further current understanding regarding regional environmental changes as a response to global climate change.

The Badain Jaran Desert, located in the arid region of northwestern (NW) China, lies in the climatic transition zone between the Asian summer monsoon and the westerly belt. This region is sensitive to climate change and is of great significance for discussing the interaction between the Asian summer monsoon and westerly circulation systems and its impact on the regional climate (Yang et al., 2003, 2010; Li et al., 2015b, 2018; Wang et al., 2016; Chen et al., 2019). A total of 110 closed inland lakes lie between megadunes in the southeastern desert (Wang et al., 2016). In previous studies, researchers have reconstructed lake evolution and discussed effective moisture changes based on these lake shorelines (Wang et al., 2016) and sediments (Chen et al., 2019; Ning et al., 2019). However, lakes in the desert hinterland are mainly recharged by groundwater and not by river runoff (Dong et al., 2016; Wang et al., 2016). Therefore, it is unclear whether these local lake-level fluctuations in the desert hinterland were sensitive to the climate change between arid and humid environments during the Holocene. Therefore, reconstructing millennial-scale precipitation and effective moisture changes is useful for addressing these questions.

Calcareous root tubes (CRTs), also called rhizoliths, are pedogenic carbonate encrustations produced by roots and microorganisms in calcareous soils or in eolian deposits in the rhizosphere of terricolous plants (Klappa, 1980; Li et al., 2015b; Zamanian et al., 2016). CRTs are widely distributed in the desert (Li et al., 2015a). Yang (2000) first used radiocarbon methods to date the CRTs and

*Corresponding author at: College of Earth and Environmental Sciences, Center for Glacier and Desert Research, Lanzhou University, 730030 Lanzhou, China. E-mail address: lizhuolunlzl@163.com; zhll@lzu.edu.cn (Z. Li).

Cite this article: Li Z, Li X, Dong S, Gao Y (2022). Holocene climate background for lake evolution in the Badain Jaran Desert of northwestern China revealed by proxies from calcareous root tubes. *Quaternary Research* **110**, 1–12. https://doi.org/10.1017/qua.2022.31

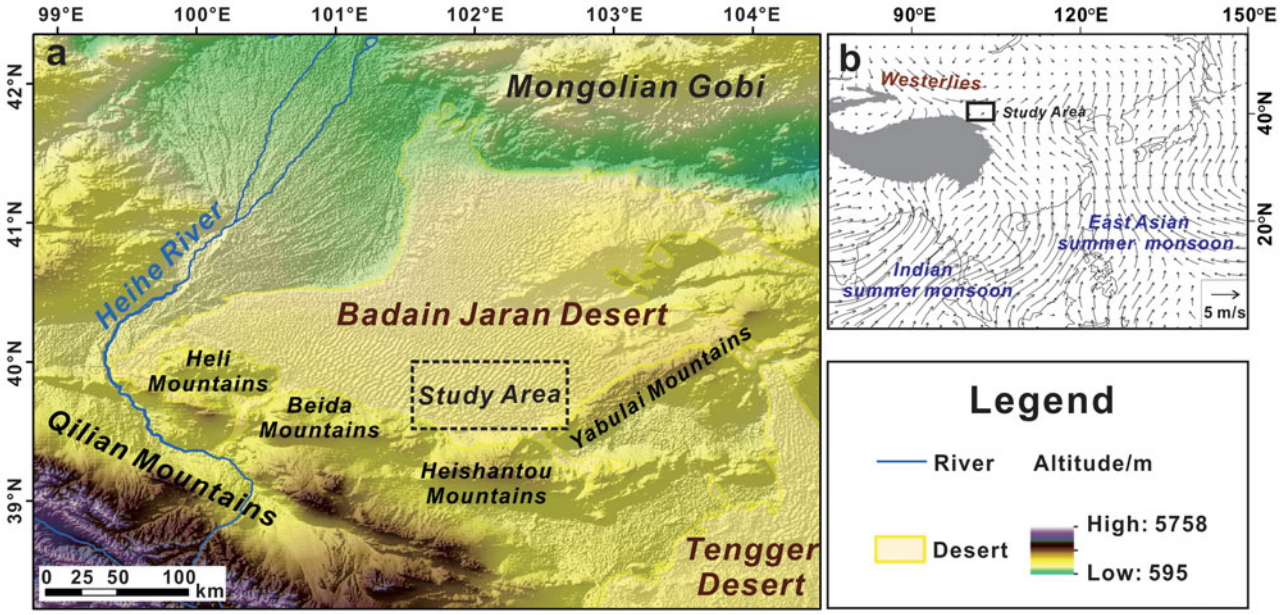

Figure 1. Overview map showing the study area and atmospheric circulation system: (a) location of the study area; (b) atmospheric circulation system: arrow shows 70-year mean summer (June, July, August) wind streamline (1000 hPa) based on National Centers for Environmental Prediction/National Center for Atmospheric Research (NCEP/NCAR) reanalysis data from 1948 to 2016.

discussed the landscape evolution and precipitation changes in the desert. In contrast to lakes in the desert hinterland, which are affected by groundwater flows, the formation of CRTs is mainly controlled by changes in soil moisture, which is affected by precipitation and evaporation but not by groundwater (Li et al., 2015a, 2015b; Gao et al., 2019; Zhu et al., 2019). Moreover, ^{14}C carbonate dating for Holocene CRTs is reliable at the millennial scale (Kuzyakov et al., 2006; Pustovoytov et al., 2007; Gocke et al., 2011; Li et al., 2020b). As a result, CRTs have been considered a suitable material for reconstructing paleoenvironmental changes in the deserts of NW China (Li et al., 2020b). They have been used in numerous paleoenvironmental reconstructions of effective moisture, precipitation, and paleovegetation (Li et al., 2017; Gao et al., 2019, 2020b). Among these, Mg/Ca ratio is viewed as a proxy of effective moisture (Gao et al., 2019), and phytolith assemblages can be used to reconstruct mean annual precipitation (MAP) quantitatively at the millennial scale during the Holocene (Gao et al., 2020b). However, such methods have not previously been applied in the Badain Jaran Desert to reconstruct such changes.

In this study, 10 Holocene CRT samples were collected from the southeastern region of the Badain Jaran Desert, and effective moisture and precipitation changes during the Holocene were reconstructed from the CRTs. We then compared the results with the evolution of the groundwater-recharged lake to clarify whether the lake-level fluctuations are sensitive to climate change between arid and humid environments.

STUDY AREA

The Badain Jaran Desert (39°04′–42°12′N, 99°23′–104°34′E) is located in the western part of the Alashan Plateau of NW China (Fig. 1), covering an area of 52,100 km^2 with an elevation of 900–1500 m (Zhu et al., 2010). It is characterized by a strong continental climate (Xu and Li, 2016; Li et al., 2020a). In this desert area, the mean annual temperature ranges from 8.8°C to 9°C (Li et al., 2018). Precipitation occurs predominantly in summer (from June to August), and the annual average precipitation is approximately 35–115 mm, which decreases markedly from southeast to northwest across the region (Ma et al., 2011). The annual evaporation from water surfaces is more than 1000 mm, far outpacing precipitation (Yang et al., 2010; Li et al., 2016a).

There are 110 perennial closed inland lakes lying between megadunes in the southeastern Badain Jaran Desert, and most of these lakes have a surface area of less than 1 km^2 (Wang et al., 2016). There are also more than 50 springs in the desert, mostly near the lakes (Dong et al., 2016). Precipitation observation in this area revealed that local atmospheric precipitation does not contribute significantly to groundwater recharge (Ma et al., 2014). Thus, due to the extremely low precipitation and high potential evaporation, inland lakes in the desert hinterland are mainly recharged by groundwater (Yang et al., 2010; Dong et al., 2016; Jin et al., 2018). The southern-central groundwater flow system in the Badain Jaran Desert originates from meltwater from the Qilian Mountains (Zhao and Li, 2018; Yi et al., 2020). Fresh groundwater emerges under pressure from the lake bottom and/or springs and is supplied to the lakes (Wang et al., 2016).

The vegetation of the desert is dominated by xerophytic and ultra-xerophytic shrubs, semishrubs, and annual herbs. Some halophytes are distributed around the lake basins (Wang et al., 2015).

MATERIALS AND METHODS

Sample collection

The evolution of some of the lakes in the southeast area of the Badain Jaran Desert (Fig. 2) during the Holocene has previously been reconstructed (Yang et al., 2010; Wang et al., 2016; Chen et al., 2019; Ning et al., 2019). In this region, CRTs are mainly scattered horizontally on the surfaces of the sand layers at

https://doi.org/10.1017/qua.2022.31 Published online by Cambridge University Press

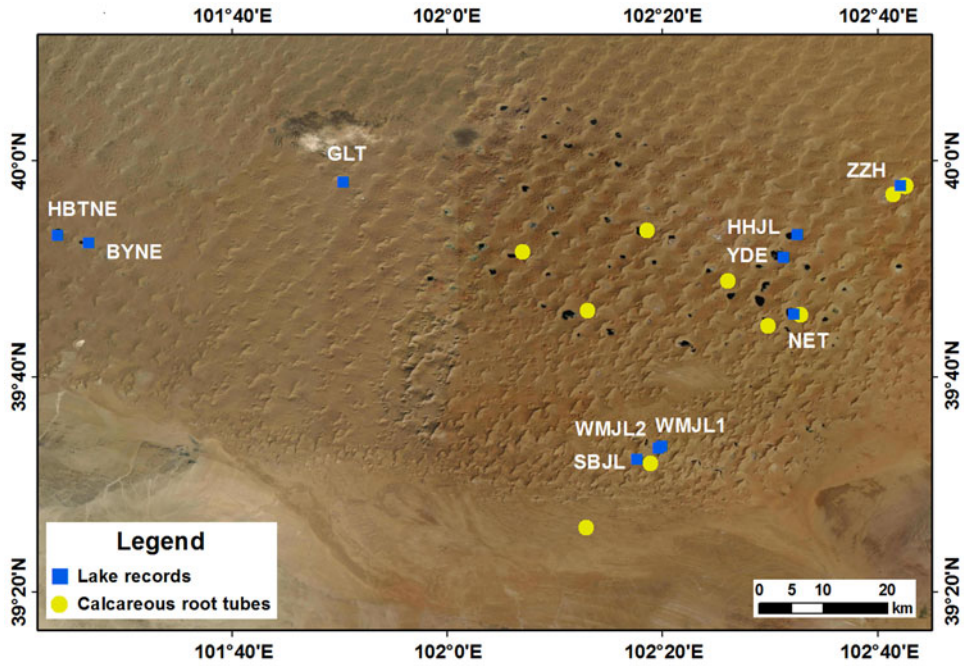

Figure 2. Locations of the Holocene calcareous root tubes (CRTs) sampled and lake records from the southeastern Badain Jaran Desert. Yellow dots indicate the Holocene CRT sample locations in the Badain Jaran Desert. Blue squares are the high lake-level records from previous studies. These records are abbreviated as follows: HBTNE, Habutenuoer (Wang et al., 2016); BYNE, Bayannuoer (Wang et al., 2016); GLT, Gailite (Wang et al., 2016); ZZH, Zhunzhahanjilin (Ning et al., 2019); HHJL, Huhejilin (Yang and Williams, 2003); YDE, Yindeer (Chen et al., 2019); NET, Nuoertu (Yang et al., 2010); WMJL1 and 2, Womenjilin 1 and 2 (Chen et al., 2019); SBJL, Shaobaijilang (Yang et al., 2010).

different altitudes of the megadunes (Fig. 3a). These CRTs record regional precipitation and effective moisture conditions in the desert (Li et al., 2015b). In the swale around the interdune lakes, the soil moisture content was previously found to be higher than in the megadunes and interdune depressions. CRTs located in these areas usually contain local soil moisture, which is unsuitable for regional paleoclimate reconstruction studies (Li et al., 2015b; Sun et al., 2021). Therefore, we collected CRT samples at different elevations of the megadunes (Fig. 2). The proxy records from these samples may indicate regional climatic conditions. The spatial distribution of the sample sites is consistent with the location of most of the perennial lakes, as can be seen in the remote sensing image (Fig. 2).

Most CRTs have a tubular morphology with a central void formed by the cementation of white carbonate minerals, predominantly calcite (Fig. 3b). The CRTs vary in length from a few cm to more than 100 cm, and their diameters range from 0.2 to 3.2 cm (Fig. 3c). The surface of all sampling sites is covered by >1 m of eolian sand, which had a median sand particle size of 0.2–0.4 mm.

Chronology

The results of ^{14}C dating of pedogenic carbonate can be affected by various factors, such as recrystallization and incorporation of older and younger carbon (Gocke et al., 2011; Li et al., 2020b). The carbon source for CRTs is a mixture of soil CO_2 derived from root respiration and atmospheric CO_2 (Gao et al., 2020a). Li et al. (2015a) determined that the incorporation of older carbon slightly influenced ^{14}C ages for CRT samples from the Badain Jaran Desert. The age difference between the CRTs and aquatic mollusk shells from the desert was less than 300 years, indicating that the Holocene ^{14}C dates for the CRTs are robust at the millennial scale (Li et al., 2015a). This is consistent with the results previously reported by Pustovoytov et al. (2007) and Gocke et al. (2011). Li et al. (2020b) showed that the inner precipitated carbonate layer of the CRTs was not affected by recrystallization. Therefore, carbonate from the inner belt of CRTs is a suitable material for ^{14}C dating.

In this study, we collected carbonate from the inner belt of five recently collected CRT samples, which were then dated via accelerator mass spectrometry (AMS) radiocarbon analysis. During pretreatment, ultrasonic cleaners were used to remove small amounts of carbonate attached to the exteriors of the CRT samples. AMS ^{14}C dating was conducted at the Laboratory of Scientific Archaeology and Preservation of Cultural Relics, School of Archaeology and Museology, Peking University, China. All radiocarbon ages were converted to calendar year ages using the IntCal20 model of the Calib 8.2 program (Reimer et al., 2020).

Major elements analysis

The concentrations of major elements in our bulk samples of CRTs were determined by X-ray fluorescence (XRF) spectrometry at the Key Laboratory of Western China's Environmental System, Lanzhou University. The samples were powdered and sifted through a 200-mesh screen, and 4 g of each sample was poured into the center of a column apparatus with boric acid and pressurized for 20 s using the YYJ-40 semiautomatic oil hydraulic apparatus. The compressed samples were approximately 4 cm in diameter and 0.8 cm thick. They were then measured by XRF spectrometry (Panalytical Magix PW2403, Netherlands).

Analytical results for major elements were reported in the form of oxide compound concentrations. The accuracy and precision of the result of the XRF method met the analysis

https://doi.org/10.1017/qua.2022.31 Published online by Cambridge University Press

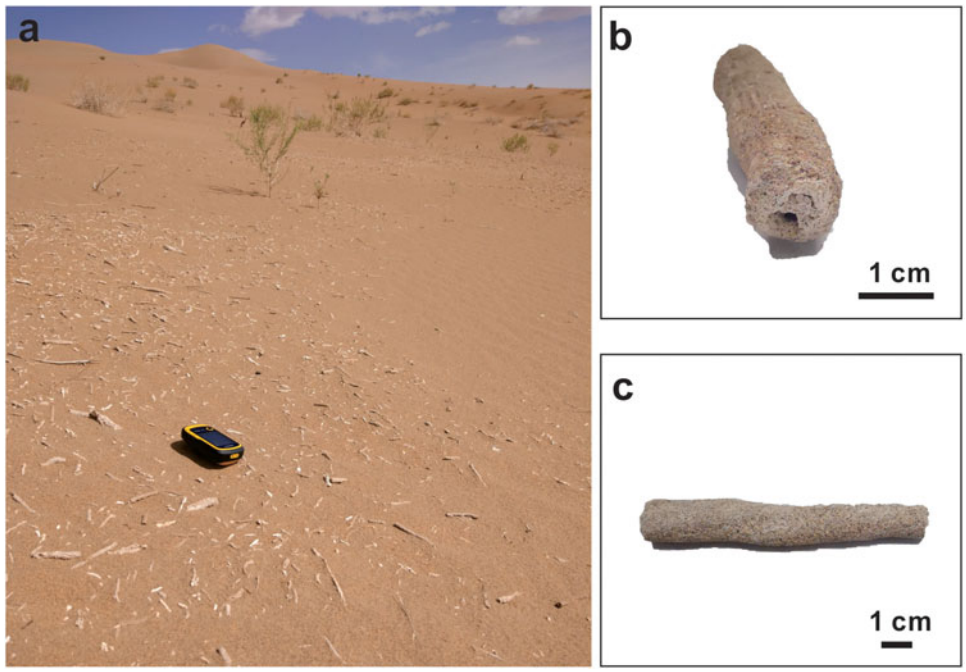

Figure 3. Distribution and morphology of calcareous root tubes (CRTs) in the Badain Jaran Desert: (a) CRTs are scattered horizontally on the surfaces of sand layers at different altitudes of the megadunes; (b and c) morphological characteristics of CRTs.

requirements, which have been described by Gao et al. (2019). The results of element analysis for the samples were compared with standard values from GBW07401 (GSS-1). The repeatability for major element analysis was estimated by the standard deviation of triplicate measurements. The standard deviations were <4% for CaO and MgO.

Phytolith extraction and classification

Phytolith extraction from CRTs followed the wet ashing procedure, as reported in Gao et al. (2020b). Phytolith counting and identification were performed using a microscope (Shanghai Changfang Optical Instrument Co., China) at 400× magnification. Each sample contained more than 300 phytoliths. Phytolith abundance was described as a percentage of the total number of phytoliths. The phytoliths were divided into 14 types based on the classification systems of several previous studies (Twiss et al., 1969; Lu et al., 2006, 2007; Gao et al., 2020b) and international phytolith nomenclature (ICPN2.0; ICPT, 2019) (Fig. 4). The corresponding ICPN2.0 nomenclature is placed in brackets after each morphotype: (1) dumbbell (BILOBATE), (2) short-saddle (SADDLE), (3) wavy-narrow-trapezoid (TRAPEZOID), (4) rondel (RONDEL), (5) fan-reed (BULLIFORM FLABELLATE), (6) fan (BULLIFORM FLABELLATE), (7) square (BLOCKY), (8) rectangle (TABULAR ENTIRE), (9) board-elongate (ELONGATE ENTIRE), (10) sinuate-elongate (ELONGATE SINUATE), (11) smooth-elongate (ELONGATE ENTIRE), (12) long-point (ACUTE BULBOSUS), (13) short-point (ACUTE BULBOSUS), and (14) gobbet (BLOCKY).

Effective moisture and quantitative precipitation reconstructions

The Mg/Ca ratio in CRTs is considered a proxy for effective moisture (Gao et al., 2019). In arid regions, the transport of soil solutions may trigger CO_2 degassing under high evaporation rates, promoting prior calcite precipitation (McDonald et al., 2004; Cruz et al., 2007). Thus, according to the Rayleigh distillation, the correlation between the Mg/Ca ratio and residual Ca in soil solution is negative (Gao et al., 2019). Therefore, a higher effective moisture and soil water content in the desert would result in higher actual evaporation and more Ca would be precipitated from the soil solution, resulting in an increase in the Mg/Ca ratios in the residual soil solution and an increase in the Mg/Ca ratios in the CRTs (Gao et al., 2019). Accordingly, a higher Mg/Ca ratio corresponds to higher effective moisture, and vice versa (Gao et al., 2019; Zhu et al., 2019). Recrystallization occurring in the CRT detrital layer may result in geochemical changes in the bulk CRT samples (Li et al., 2020b). However, this has little effect on paleoenvironmental reconstruction results when the Mg/Ca ratios in CRTs are used as a proxy (Li et al., 2020b).

Phytoliths are noncrystalline SiO_2 minerals deposited in and between plant cells that can be preserved in soil and sediment for long periods after plants die and decay (Webb and Longstaffe, 2000; Piperno, 2006; Zuo et al., 2021). Some plants produce distinctive and diagnostic phytolith types that can indicate special climatic conditions (Wang and Lu, 1993; Prebble et al., 2002; Esteban et al., 2017). Phytoliths from surface soil samples have already revealed that the distribution of some common phytolith types was affected by climatic conditions (Strömberg, 2004; Lu et al., 2006; Biswas et al., 2021). In warm and humid conditions, some phytolith types such as square, rectangle, and fan types have high percentages; whereas in cold and arid conditions, elongate, point, trapezoid, and rondel phytolith types have high percentages (Wang et al., 2003; Zuo et al., 2021). Therefore, phytolith assemblages from various archives have been used to reconstruct paleoclimates (Horrocks et al., 2000; Blinnikov et al., 2002; Carter, 2002; Zuo et al., 2016; Liu et al., 2019). Phytoliths within CRTs originated from local surface vegetation during CRT formation (Gao et al., 2020b). Using the phytolith-precipitation transfer function, phytolith assemblages can be

https://doi.org/10.1017/qua.2022.31 Published online by Cambridge University Press

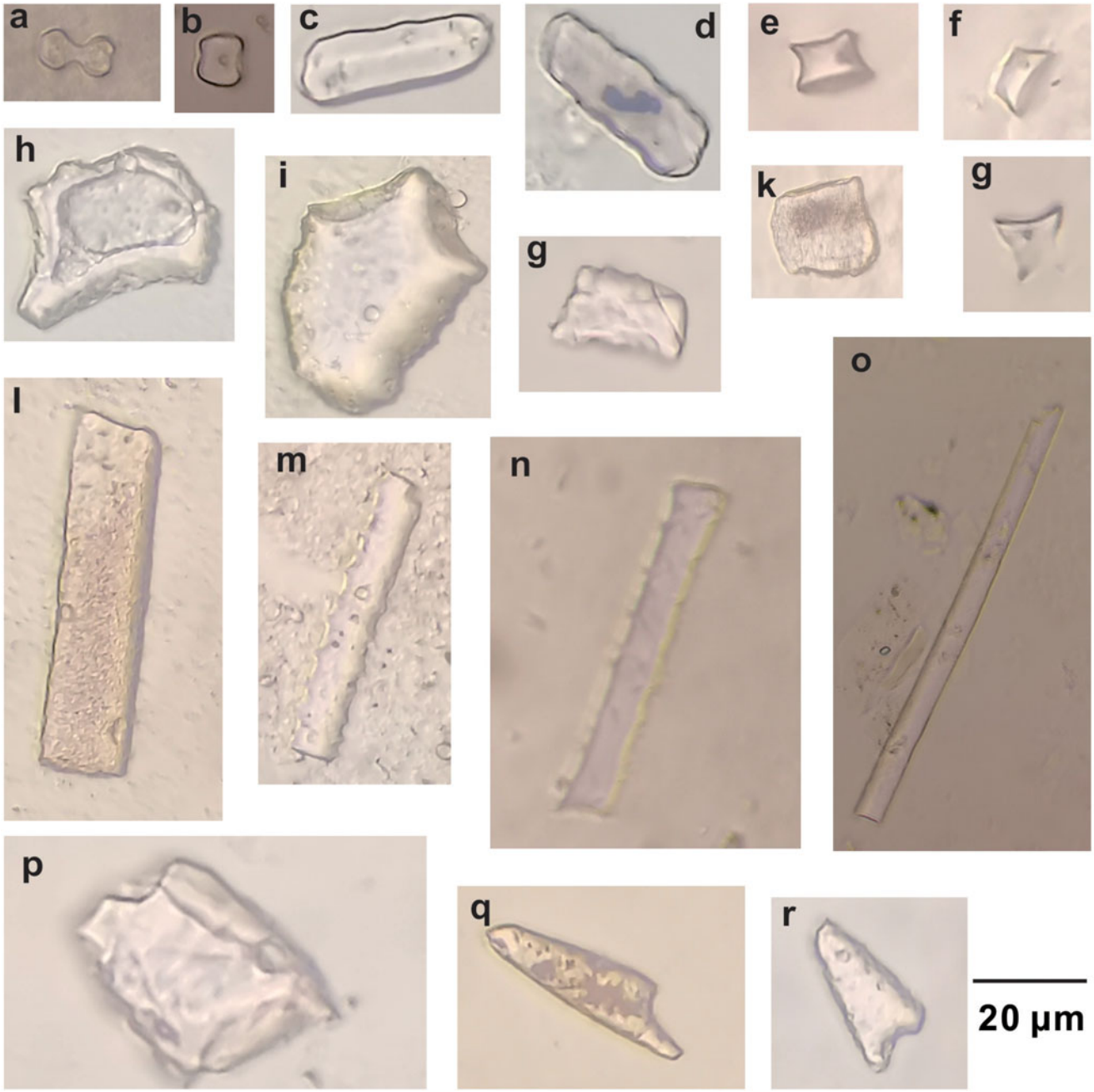

Figure 4. Phytolith morphotypes identified from the CRT samples in the Badain Jaran Desert. The ICPN2.0 nomenclature is placed within brackets after each morphotype: (a) dumbbell (BILOBATE), (b) short-saddle (SADDLE), (c and d) wavy-narrow-trapezoid (TRAPEZOID), (e–g) rondel (RONDEL), (h) fan (BULLIFORM FLABELLATE), (i) fan-reed (BULLIFORM FLABELLATE), (j) rectangle (TABULAR ENTIRE), (k) square (BLOCKY), (l) board-elongate (ELONGATE ENTIRE), (m and n) sinuate-elongate (ELONGATE SINUATE), (o) smooth-elongate (ELONGATE ENTIRE), (p) gobbet (BLOCKY), (q) long-point (ACUTE BULBOSUS), and (r) short-point (ACUTE BULBOSUS).

used to reconstruct Holocene millennial-scale precipitation (Lu et al., 2006; Gao et al., 2020b).

The transfer function method used 238 surface-sediment samples along broad ecological and climatic gradients across China as the training set (Lu et al., 2006). MAP values were inferred quantitatively using a unimodal response model in R with the rioja package, which is based on weighted-average partial least squares regression and calibration (ter Braak and Juggins, 1993) using C^2 v. 1.3 (Juggins, 2003). The results showed that phytoliths provide robust estimates of MAP ($R^2_{\text{boot}} = 0.90$, root mean-square error of prediction = 148 mm). Then, to clarify whether the training set from the whole of China could be applied to arid or semiarid areas, the 30 sites within the surface-sediment training set from Lu et al. (2006) were used in the model to simulate results with precipitation of less than 300 mm. There was a relatively high correlation coefficient between the simulated MAP and the deviation ($y = 0.747^*x - 95.520$, $R^2 = 0.622$, $P < 0.01$) (Gao et al., 2020b), which can be used for model correction of Lu et al. (2006). After optimization, the new standard errors of the quantitative

https://doi.org/10.1017/qua.2022.31 Published online by Cambridge University Press

Table 1. ^{14}C dates for the Holocene CRT samples collected in the Badain Jaran Desert.

Lab. no.	Latitude/N	Longitude/E	^{14}C yr BP	cal yr BP (2σ)[a]	References
BA110772	39°46′7.90″	102°28′34.8″	4585 ± 35	5253 (5451–5054)	Li et al., 2015a
LUG11-195	39°56′13.9″	102°36′20.1″	5564 ± 66	6353 (6490–6215)	Li et al., 2015a
LUG11-186	39°56′56.6″	102°37′23.4″	6843 ± 65	7703 (7830–7575)	Li et al., 2015a
LUG13-52	39°51′27.13″	102°05′15.44″	2482 ± 50	2545 (2724–2366)	Li et al., 2017
LUG13-53	39°46′29.41″	102°10′42.45″	3071 ± 51	3238 (3393–3082)	Li et al., 2017
BA181193	39°53′13.37″	102°15′44.27″	5290 ± 35	6066 (6189–5942)	This study
BA181194	39°49′01.35″	102°22′29.63″	4435 ± 25	5077 (5276–4878)	This study
BA181195	39°45′12.95″	102°25′51.32″	5005 ± 25	5749 (58895608–)	This study
BA181197	39°33′46.2″	102°14′59.9″	4970 ± 25	5673 (5744–5602)	This study
BA181198	39°28′21.89″	102°10′35.78″	4025 ± 25	4495 (4570–4419)	This study

[a]The calibrated ^{14}C ages (2σ) were all calculated using Calib v. 8.2 (http://calib.org/calib/calib.html).

precipitation reconstruction results were between 37 and 39 mm. This transfer function has been confirmed as suitable when using phytolith assemblages from CRTs in this region to quantitatively reconstruct Holocene millennial-scale precipitation (Gao et al., 2020b).

In this study, the transfer functions were applied to 10 phytolith assemblages from CRTs in the desert. First, phytolith assemblages from 238 surface-sediment sites were used for model training (Lu et al., 2006). Second, quantitative precipitation reconstructions of the desert were achieved using the rioja package in R (Juggins, 2003). Finally, the regression equation of Gao et al. (2020b) ($y = 0.747^{*}x - 95.520$) was used to optimize the reconstructed MAP.

RESULTS

^{14}C dating

We have dated 21 CRT samples from the Badain Jaran Desert in our previous studies (Li et al., 2015a; Li et al., 2017) and this study. According to radiocarbon dating, 11 CRT samples dated to the late Pleistocene (Li et al., 2015a), and 10 samples dated to the Holocene. The ^{14}C dating results of the 10 Holocene CRT samples (Fig. 2; Table 1) yielded a range of dates, with one sample older than 7000 cal yr BP, six samples dated to 7000–5000 cal yr BP, and three samples dated to 5000–2000 cal yr BP (Table 1).

Mg/Ca ratio variation and effective moisture reconstruction

XRF results revealed that the Mg/Ca ratio values had fluctuated between 7000 and 5000 cal yr BP, with an average ratio value of 0.058 mol/mol (Fig. 5). Although the Mg/Ca ratio increased slightly between 5000 and 2000 cal yr BP, with an average of 0.043 mol/mol, it remained significantly lower than the values at 7000–5000 cal yr BP (Fig. 5). Thus, based on the environmental significance of the Mg/Ca ratio, higher effective moisture conditions occurred during 7000–500 cal yr BP and lower effective moisture conditions during 5000–2000 cal yr BP.

Phytolith assemblage variation and quantitative precipitation reconstruction

The 14 phytolith types and the variations in abundance in the 10 CRT samples are summarized in Figures 4 and 6. The major phytolith types included smooth-elongate, gobbet, short-saddle, square, short-point, long-point, rondel, rectangle, wavy-narrow-trapezoid, and fan types. The relative abundance of these types was higher than 1%. The phytolith assemblage characteristics and quantitative precipitation reconstructions in the Badain Jaran Desert during the Holocene are described in the following paragraphs.

Stage 1 (before 7000 cal yr BP): The phytolith assemblages were dominated by gobbet types (23%). The percentage contents of rondel (17%), short-saddle (15%), short-point (14%), smooth-elongate

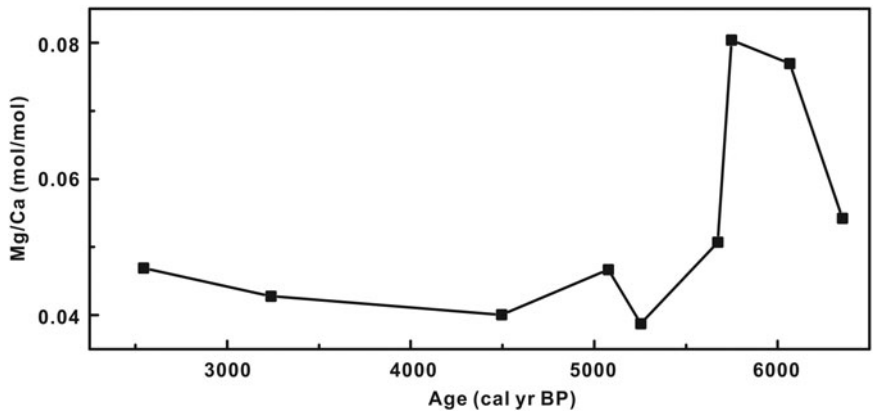

Figure 5. Changes in Mg/Ca ratio from calcareous root tubes (CRTs) in the Badain Jaran Desert during 7000–2000 cal yr BP.

https://doi.org/10.1017/qua.2022.31 Published online by Cambridge University Press

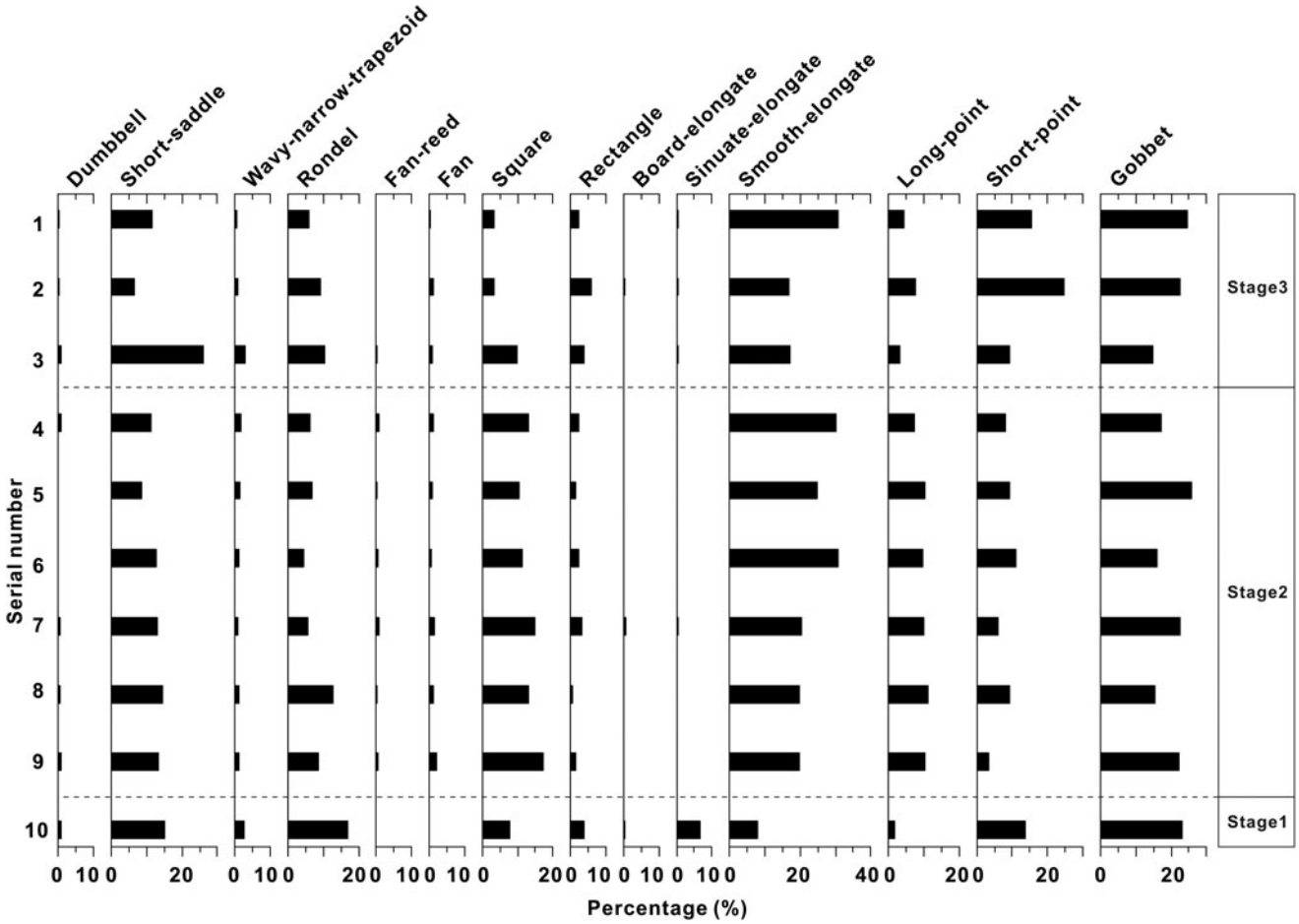

Figure 6. Relative abundance of phytoliths observed from calcareous root tube (CRT) samples in the Badain Jaran Desert. Stages 1, 2, and 3 indicate before 7000 cal yr BP, 7000–5000 cal yr BP, and 5000–2000 cal yr BP, respectively.

(8%), square (8%), and sinuate-elongate (7%) types were relatively high, whereas the percentage contents of rectangle (4%), wavy-narrow-trapezoid (3%), and long-point (2%) types were relatively low (Fig. 6). The relative abundance of the other types was less than 1% (Fig. 6). The distribution of phytolith assemblages reflected a relatively arid climate. Based on the phytolith–precipitation transfer function, the reconstructed MAP was 154 ± 38 mm during this period (Fig. 7).

Stage 2 (7000–5000 cal yr BP): The phytolith assemblages were dominated by smooth-elongate (23 ± 5%) and gobbet (19 ± 4%) types. The percentage contents of short-saddle (14 ± 6%), square (13 ± 3%), long-point (9 ± 3%), short-point (8 ± 3%), and rondel (8 ± 3%) types were relatively high, whereas rectangle (2 ± 1%), wavy-narrow-trapezoid (1 ± 1%), and fan (1 ± 1%) types were relatively low (Fig. 6). The relative abundance of the other types was less than 1% (Fig. 6). The distribution of phytolith assemblages reflected a relatively humid climate. Based on the phytolith–precipitation transfer function, the reconstructed MAP was 175 ± 37 to 205 ± 37 mm during this period (Fig. 7).

Stage 3 (5000–2000 cal yr BP): The phytolith assemblages were also dominated by smooth-elongate (24 ± 10%) and gobbet (24 ± 2%) types, but relative abundance increased compared with stage

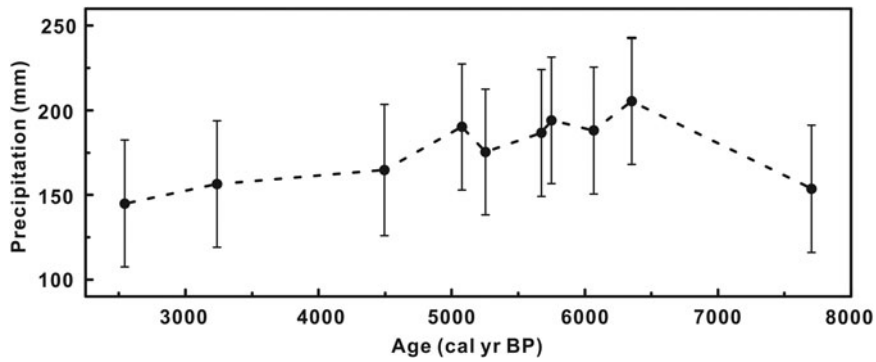

Figure 7. Phytolith-based quantitative reconstructions of millennial-scale precipitation changes in the Badain Jaran Desert during the Holocene.

https://doi.org/10.1017/qua.2022.31 Published online by Cambridge University Press

2 (Fig. 6). The percentage of short-point types (20 ± 7%) increased significantly, whereas the short-saddle (9 ± 4%), rondel (8 ± 2%), long-point (6 ± 2%), and square (3 ± 1%) types declined (Fig. 6). The percentage of rectangle types (4 ± 3%) increased slightly (Fig. 6). The relative abundance of the other types was less than 1% (Fig. 6). The distribution of phytolith assemblages reflected a relatively arid climate compared with the period between 7000 and 5000 cal yr BP. Based on the phytolith–precipitation transfer function, the reconstructed MAP was 145 ± 37 to 165 ± 39 mm (Fig. 7).

DISCUSSION

Comparison of climate change and lake evolution

Relatively high effective soil moisture is conducive to the formation of CRTs and was a controlling factor for CRT formation in the Badain Jaran Desert (Li et al., 2015a). The distribution frequency of CRTs showed relatively few CRTs before 7000 cal yr BP (Li et al., 2015b), which indicates an relatively arid environment with low effective soil moisture that was not suitable for the formation of CRTs. The MAP was approximately 154 ± 38 mm during this period (Fig. 7). Moreover, in the Tengger Desert, located to the southeast of the Badain Jaran Desert (Fig. 1), a low frequency of CRT distribution occurred in the corresponding period (Li et al., 2015b). The quantitative reconstruction of precipitation showed that the MAP in the period 10,000–7000 cal yr BP (138 ± 16 to 149 ± 18 mm) was 40 mm less than in the period 7000–5000 cal yr BP (179 ± 26 to 192 ± 26 mm) (Gao et al., 2020b). In addition, the accumulation of loess on the southeastern margin of the Badain Jaran Desert also indicated low effective moisture during this period (Gao et al., 2006). These results are evidence of a relatively arid climate before 7000 cal yr BP.

A millennial-scale climate reconstruction of the Badain Jaran Desert suggested a relatively humid climate during 7000–5000 cal yr BP, and the MAP was 175 ± 37 to 205 ± 37 mm (Fig. 8a and b). During 5000–2000 cal yr BP, the effective moisture was low, with a MAP of 145 ± 37 to 165 ± 39 mm (Fig. 8a and b), and the climate became relatively arid.

However, Holocene lake evolution in the Badain Jaran Desert is not fully consistent with our effective moisture and precipitation reconstruction results (Fig. 8). Previous studies revealed that the lake levels were relatively high during the Early and Middle Holocene. In the southeastern margin of the desert (Yang et al., 2003, 2010), at 10,000–4000 cal yr BP, the water levels of the lakes were approximately 2–15 m above the present water level (Fig. 8c). The quantitative reconstruction of the consecutive paleolake-level fluctuations from the Zhunzhahanjilin (ZZH) section indicated that high lake levels occurred between

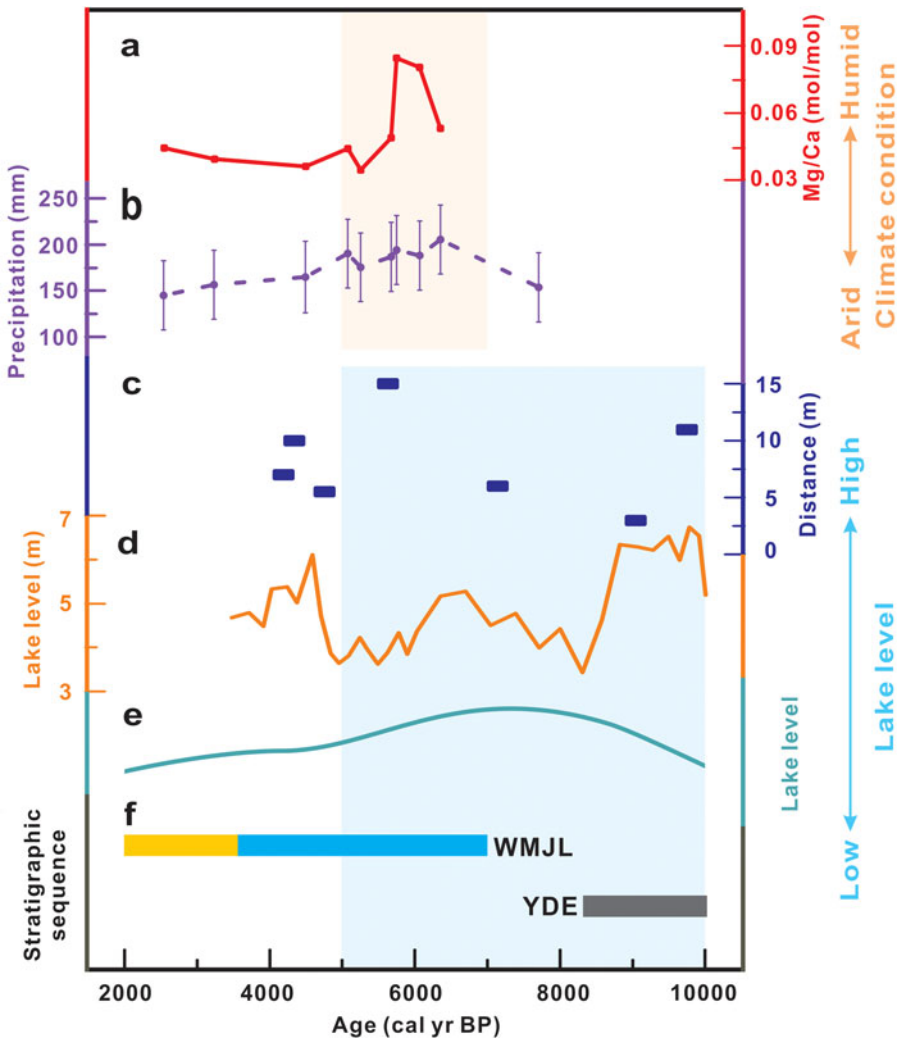

Figure 8. The comparison of climate changes and lake evolution in the Badain Jaran Desert during the Holocene: (a) changes in Mg/Ca ratio from calcareous root tubes (CRTs) at the millennial scale (this study); (b) quantitative precipitation reconstructions revealed by phytolith assemblages (this study); (c) lake-level elevation above the present water surface (Yang et al., 2010), the record contained Huhejilin, Nuoertu, and Shaobaijilang lakes; (d) the quantitatively reconstructed consecutive paleolake-level fluctuations from Zhunzhahanjilin (ZZH) section (Dong et al., 2022); (e) high lake levels during the Holocene in the Badain Jaran Desert, including records for Habutenuoer (HBTNE), Bayannuoer (BYNE), and ZZH lakes (Wang et al., 2016); and (f) stratigraphic sequence for the Yindeer (YDE) and Womenjilin (WMJL) sections in the Badain Jaran Desert (Chen et al., 2019): orange represents eolian deposits, blue represents lacustrine deposits, and gray represents gyttja deposits. The pink shadow indicates the humid climate during the Middle Holocene. The blue shadow indicates the lakes with high levels during the Early and Middle Holocene.

https://doi.org/10.1017/qua.2022.31 Published online by Cambridge University Press

10,600–4700 cal yr BP with fluctuations of 3.41–9.21 m (Dong et al., 2022). Wang et al. (2016) revealed that many lakes in the desert hinterland reached their maximum water levels during the period 8600–6300 cal yr BP (Fig. 8e). Moreover, Chen et al. (2019) proposed that lakes were developing in the desert during the period 10.7–3.6 ka (Fig. 8f). The incomplete synchronization between lake evolution and climate change indicates that lake evolution may be influenced not only by climatic factors but also by non-climatic factors.

Factors influencing lake evolution in the Badain Jaran Desert

Fluctuations in the depths and areas of inland lakes usually provide significant evidence of the water budget, which is directly linked to atmospheric precipitation. However, there is a different water budget for lakes located in the desert hinterlands and other inland regions. First, there was no direct surface runoff flowing into the lakes in the Badain Jaran Desert hinterland (Dong et al., 2016). Second, there is evidence that atmospheric precipitation did not contribute significantly to the groundwater system (Ma et al., 2014). Third, measures of evaporation and estimated water balance indicate that groundwater recharge contributed a much greater portion of the total lake replenishment (Dong et al., 2016; Sun et al., 2018). As a result, the amount of groundwater recharge drives changes in lake levels in the desert hinterland (Wu et al., 2014; Dong et al., 2016). Although there is an ongoing debate regarding the origin of groundwater (Yang et al., 2003; Chen et al., 2004; Ma and Edmunds, 2006; Gates et al., 2008; Shao et al., 2012; Dong et al., 2016), deep phreatic water is likely the main replenishment source. Therefore, lake-level fluctuations in the desert must be influenced by a combination of atmospheric precipitation, evaporation, and groundwater recharge.

During the Holocene, lake levels in the study area increased before 7000 cal yr BP (Yang et al., 2003, 2010; Wang et al., 2016), but the precipitation was relatively low, resulting in a relatively arid climate. At the same time, high solar insolation resulted in high temperatures (Berger and Loutre, 1991), which could have led to increased evaporation. This climate condition was not beneficial for the lake-level increase. Thus, the high lake levels during this period were probably influenced by the increase in groundwater recharge. High temperatures could increase meltwater in the lake recharge areas, such as the Qilian Mountains and the Qinghai-Tibet Plateau, which recharged the lakes with groundwater, causing a rise in lake levels in the desert hinterland. Li et al. (2016b) have shown that abundant runoff occurred in the western Qilian Mountains during the Early Holocene (10,500–8800 cal yr BP). Wünnemann et al. (2012) also suggested that, in the case of Hala Lake in the period between 10,000 and 9500 cal yr BP, stepwise lake-level rise was most likely a response to intense glacier melt in the Qilian Mountains. Moreover, there is also evidence of meltwater from glaciers resulting in abundant runoff and lake-level rise in the Qinghai-Tibet Plateau (Gyawali et al., 2019; Hou et al., 2021). These studies provide evidence of abundant meltwater before 7000 cal yr BP. Thus, a rise in lake levels before 7000 cal yr BP can be attributed to an increase in meltwater transformed to groundwater, which then recharged the lakes.

In the present study, quantitative precipitation reconstruction results showed that the MAP reached 175 ± 37 to 205 ± 37 mm in the period 7000–5000 cal yr BP, which is approximately twice the current precipitation level. During this period, many lakes reached their highest levels (Yang et al., 2003, 2010, 2011; Wang et al., 2016; Chen et al., 2019), and evaporation decreased with the decline in solar insolation (Berger and Loutre, 1991). Our results also revealed a humid environment with high effective moisture and precipitation during this period (Fig. 8). Therefore, the lake-level fluctuations were consistent with the effective moisture and precipitation at 7000–5000 cal yr BP. However, whether the increase in groundwater recharge led to synchronous increases in lake levels requires further study.

After 5000 cal yr BP, precipitation and effective moisture decreased (Fig. 8a and b), resulting in an arid environment. Under these circumstances, lake levels declined (Yang et al., 2010, 2011; Wang et al., 2016; Chen et al., 2019).

Thus, lake evolution in the desert hinterland during the Holocene was influenced by precipitation, evaporation, and groundwater recharge. Before 7000 cal yr BP, lake-level rise can be attributed to an increase in meltwater flowing into the groundwater in the lake recharge areas. In other periods, lake-level fluctuations are sensitive to climate change between arid and humid environments.

Mechanisms possibly forcing climate changes

The study area is located in the Asian monsoon margin of NW China (Li et al., 2020a). In this region, precipitation and effective moisture changes at the millennial scale during the Holocene differed from those observed in the typical monsoon region (Li et al., 2015b; Gao et al., 2020a, 2020b). Precipitation during the Early and Middle Holocene in this region was affected by changes in the northernmost margin of the Asian summer monsoon (Lu et al., 2005; Gao et al., 2020b).

Before 7000 cal yr BP, with increased insolation (Berger and Loutre, 1991), the Asian summer monsoon reached its greatest intensity (Dykoski et al., 2005; Wang et al., 2005). However, because of the suppression of the high-latitude ice sheet (Dyke, 2004; Peltier, 2004), the global sea level was lower during this period. The East Asian continental shelf was exposed to the surface, increasing the distance of moisture transported from the ocean to inland (Liu et al., 2004; Dutton and Lambeck, 2012; Li et al., 2014). Therefore, the northernmost margin of the Asian summer monsoon stalled farther south (Wen et al., 2017; Gao et al., 2020b). Furthermore, the highest temperatures occurred in the Early Holocene (Long et al., 2010), leading to increased evaporation. Therefore, the Asian monsoon margin area had an arid climate with low precipitation before 7000 cal yr BP. During the Middle Holocene, with the decline of insolation and the disappearance of the ice sheet at high latitudes around 7 ka (Peltier, 2004), the northernmost edge of the Asian summer monsoon moved northward, and monsoon precipitation increased. Moreover, low evaporation resulting from low winter solar radiation and high summer cloud cover in Central and East Asia could have led to an increase in effective moisture during this period (Li and Morrill, 2010). Therefore, a more humid environment, with higher monsoon precipitation and lower evaporation, occurred during this period.

With the decline of insolation, the intensity of the Asian summer monsoon weakened, and monsoon precipitation decreased in the Late Holocene, eventually producing a relatively arid environment.

CONCLUSIONS

Mg/Ca ratios and phytolith assemblages in Holocene CRTs from the Badain Jaran Desert were used to reconstruct changes in

https://doi.org/10.1017/qua.2022.31 Published online by Cambridge University Press

effective moisture and MAP, respectively, at the millennial scale during the Holocene. Before 7000 cal yr BP, the reconstructed MAP was 154 ± 38 mm, indicating a relatively arid environment. The effective moisture was high, with a MAP of 175 ± 37 to 205 ± 37 mm (twice the current precipitation) during 7000–5000 cal yr BP. However, the effective moisture decreased, with a MAP of 145 ± 37 to 165 ± 39 mm between 5000–2000 cal yr BP.

Holocene lake evolution in the desert is not fully consistent with effective moisture and monsoon precipitation changes. Lake-level fluctuations are influenced by precipitation, evaporation, and groundwater recharge. Before 7000 cal yr BP, the rise in lake levels can be attributed to an increase in groundwater recharge that likely originated from meltwater in the recharge area. During other periods, lake-level fluctuations were coupled with climate changes between arid and humid environments. During 7000–5000 cal yr BP, high lake levels correspond to increased monsoonal precipitation and groundwater recharge. The gradual decline of lake levels during 5000–2000 cal yr BP reflected a relatively arid climate with decreased monsoonal precipitation and groundwater recharge.

Acknowledgments. The authors thank two anonymous reviewers as well as Derek Booth and Xiaoping Yang for their constructive comments, which led to the significant improvement of this article. This study was supported by the National Natural Science Foundation of China (no. 41771211) and the Special Fund of Chinese Central Government for Basic Scientific Research Operations in Commonweal Research Institutes (no. SK202105).

REFERENCES

Berger, A., Loutre, M.-F., 1991. Insolation values for the climate of the last 10 million years. *Quaternary Science Reviews* **10**, 297–317.

Biswas, O., Ghosh, R., Agrawal, S., Morthekai, P., Paruya, D.K., Mukherjee, B., Bera, M., Bera, S., 2021. A comprehensive calibrated phytolith based climatic index from the Himalaya and its application in palaeotemperature reconstruction. *Science of the Total Environment* **750**, 142280.

Blinnikov, M., Busacca, A., Whitlock, C., 2002. Reconstruction of the late Pleistocene grassland of the Columbia basin, Washington, USA, based on phytolith records in loess. *Palaeogeography, Palaeoclimatology, Palaeoecology* **177**, 77–101.

Carter, J.A., 2002. Phytolith analysis and paleoenvironmental reconstruction from Lake Poukawa Core, Hawkes Bay, New Zealand. *Global and Planetary Change* **33**, 257–267.

Chen, J., Li, L., Wang, J., Barry, D.A., Sheng, X., Gu, W., Zhao, X., Chen, L., 2004. Water resources—groundwater maintains dune landscape. *Nature* **432**, 459–460.

Chen, T., Lai, Z., Liu, S., Wang, Y., Wang, Z., Miao, X., An, F., Yu, L., Han, F., 2019. Luminescence chronology and palaeoenvironmental significance of limnic relics from the Badain Jaran Desert, northern China. *Journal of Asian Earth Sciences* **177**, 240–249.

Cruz, F.W., Burns, S.J., Jercinovic, M., Karmann, I., Sharp, W.D., Vuille, M., 2007. Evidence of rainfall variations in southern Brazil from trace element ratios (Mg/Ca and Sr/Ca) in a Late Pleistocene stalagmite. *Geochimica et Cosmochimica Acta* **71**, 2250–2263.

Dong, C., Wang, N., Chen, J., Li, Z., Chen, H., Chen, L., Ma, N., 2016. New observational and experimental evidence for the recharge mechanism of the lake group in the Alxa Desert, north-central China. *Journal of Arid Environments* **124**, 48–61.

Dong, S., Li, Z., Li, M., Lu, C., Wang, N., Ning, K., 2022. Quantitative reconstruction of consecutive paleolake-level fluctuations by the groundwater recharged lake in the desert hinterland: a case study in the Badain Jaran Desert, Northwestern China. *Catena* **212**, 106051.

Dutton, A., Lambeck, K., 2012. Ice volume and sea level during the last interglacial. *Science* **337**, 216.

Dyke, A.S., 2004. An outline of North American deglaciation with emphasis on central and northern Canada. *Developments in Quaternary Sciences* **2**, 373–424.

Dykoski, C., Edwards, R., Cheng, H., Yuan, D., Cai, Y., Zhang, M., Lin, Y., Qing, J., An, Z., Revenaugh, J., 2005. A high resolution, absolute-dated Holocene and deglacial Asian monsoon record from Dongge Cave, China. *Earth and Planetary Science Letters* **233**, 71–86.

Esteban, I., Albert, R.M., Eixea, A., Zilhão, J., Villaverde, V., 2017. Neanderthal use of plants and past vegetation reconstruction at the Middle Paleolithic site of Abrigo de la Quebrada (Chelva, Valencia, Spain). *Archaeological and Anthropological Sciences* **9**, 265–278.

Fan, J., Xiao, J., Wen, R., Zhang, S., Huang, Y., Yue, J., Wang, X., *et al.*, 2019. Mineralogy and carbonate geochemistry of the Dali Lake sediments: implications for paleohydrological changes in the East Asian summer monsoon margin during the Holocene. *Quaternary International* **527**, 103–112.

Gao, Q., Tao, Z., Li, B., Jin, H., Zou, X., Zhang, Y., Dong, G., 2006. Palaeomonsoon variability in the southern fringe of the Badain Jaran Desert, China, since 130 ka BP. *Earth Surface Processes and Landforms* **31**, 265–283.

Gao, Y., Li, Z., Wang, N., Li, R., 2019. Controlling factors and the paleoenvironmental significance of chemical elements in Holocene calcareous root tubes in the Alashan Desert, northwest China. *Quaternary Research* **91**, 149–162.

Gao, Y., Li, Z., Zhu, R., Liao, H., 2020a. Stable isotope compositions, sources and paleoenvironmental significance of Holocene calcareous root tubes in the Tengger Desert, northwest China. *Catena* **195**, 104846.

Gao, Y., Li, Z., Zhu, R., Wang, N., 2020b. Quantitative reconstruction of Holocene millennial-scale precipitation in the Asian monsoon margin of northwest China, revealed by phytolith assemblages from calcareous root tubes in the Tengger Desert. *Climate Dynamics* **55**, 755–770.

Garcin, Y., Melnick, D., Strecker, M.R., Olago, D., Tiercelin, J.-J., 2012. East African mid-Holocene wet–dry transition recorded in palaeo-shorelines of Lake Turkana, northern Kenya Rift. *Earth and Planetary Science Letters* **331–332**, 322–334.

Gates, J.B., Edmunds, W.M., Darling, W.G., Ma, J., Pang, Z., Young, A.A., 2008. Conceptual model of recharge to southeastern Badain Jaran Desert groundwater and lakes from environmental tracers. *Applied Geochemistry* **23**, 3519–3534.

Gocke, M., Pustovoytov, K., Kühn, P., Wiesenberg, G.L.B., Löscher, M., Kuzyakov, Y., 2011. Carbonate rhizoliths in loess and their implications for paleoenvironmental reconstruction revealed by isotopic composition: $\delta^{13}C$, ^{14}C. *Chemical Geology* **283**, 251–260.

Goldsmith, Y., Broecker, W.S., Xu, H., Polissar, P.J., Demenocal, P.B., Porat, N., Lan, J., Cheng, P., Zhou, W., An, Z., 2017. Northward extent of East Asian monsoon covaries with intensity on orbital and millennial timescales. *Proceedings of the National Academy of Sciences USA* **114**, 1817–1821.

Gyawali, A.R., Wang, J., Ma, Q., Wang, Y., Xu, T., Guo, Y., Zhu, L., 2019. Paleo-environmental change since the Late Glacial inferred from lacustrine sediment in Selin Co, central Tibet. *Palaeogeography, Palaeoclimatology, Palaeoecology* **516**, 101–112.

Hartmann, K., Wünnemann, B., 2009. Hydrological changes and Holocene climate variations in NW China, inferred from lake sediments of Juyanze palaeolake by factor analyses. *Quaternary International* **194**, 28–44.

Horrocks, M., Deng, Y., Ogden, J., Sutton, D.G., 2000. A reconstruction of the history of a Holocene sand dune on Great Barrier Island, northern New Zealand, using pollen and phytolith analyses. *Journal of Biogeography* **27**, 1269–1277.

Hou, Y., Long, H., Shen, J., Gao, L., 2021. Holocene lake-level fluctuations of Selin Co on the central Tibetan plateau: regulated by monsoonal precipitation or meltwater? *Quaternary Science Reviews* **261**, 106919.

[ICPT] International Committee for Phytolith Taxonomy, 2019. International Code for Phytolith Nomenclature (ICPN) 2.0. *Annals of Botany* **124**, 189–199.

Jin, K., Rao, W., Tan, H., Song, Y., Yong, B., Zheng, F., Chen, T., Han, L., 2018. H-O isotopic and chemical characteristics of a precipitation-lake water-groundwater system in a desert area. *Journal of Hydrology* **559**, 848–860.

https://doi.org/10.1017/qua.2022.31 Published online by Cambridge University Press

Jin, M., Li, G., Li, F., Duan, Y., Wen, L., Wei, H., Yang, L., Fan, Y., Chen, F., 2015. Holocene shorelines and lake evolution in Juyanze Basin, southern Mongolian Plateau, revealed by luminescence dating. *The Holocene* **25**, 1898–1911.

Juggins, S., 2003. *C^2 User Guide: Software for Ecological and Palaeoecological Data Analysis and Visualisation*. Department of Geography, University of Newcastle, Newcastle upon Tyne, UK, pp. 1–69.

Klappa, C.F., 1980. Rhizoliths in terrestrial carbonates: classification, recognition, genesis and significance. *Sedimentology* **27**, 613–629.

Kuzyakov, Y., Shevtzova, E., Pustovoytov, K., 2006. Carbonate re-crystallization in soil revealed by ^{14}C labeling: experiment, model and significance for paleoenvironmental reconstructions. *Geoderma* **131**, 45–58.

Li, G., Li, P., Liu, Y., Qiao, L., Ma, Y., Xu, J., Yang, Z., 2014. Sedimentary system response to the global sea level change in the East China Seas since the last glacial maximum. *Earth-Science Reviews* **139**, 390–405.

Liu, H., Gu, Y., Huang, X., Yu, Z., Xie, S., Cheng, S., 2019. A 13,000-year peatland palaeohydrological response to the ENSO-related Asian monsoon precipitation changes in the middle Yangtze Valley. *Quaternary Science Reviews* **212**, 80–91.

Liu, J., Milliman, J.D., Gao, S., Cheng, P., 2004. Holocene development of the Yellow River's subaqueous delta, North Yellow Sea. *Marine Geology* **209**, 45–67.

Li, Y., Morrill, C., 2010. Multiple factors causing Holocene lake-level change in monsoonal and arid central Asia as identified by model experiments. *Climate Dynamics* **35**, 1119–1132.

Li, Z., Gao, Y., Han, L., 2017. Holocene vegetation signals in the Alashan Desert of northwest China revealed by lipid molecular proxies from calcareous root tubes. *Quaternary Research* **88**, 60–70.

Li, Z., He, Y., Chen, Q., 2018. Radiocarbon dating of aquatic gastropod shells and its significance in reconstructing Quaternary environmental changes in the Alashan Plateau of northwestern China. *Geomorphology* **318**, 18–25.

Li, Z., Pan, N., He, Y., Zhang, Q., 2016a. Evaluating the best evaporation estimate model for free water surface evaporation in hyper-arid regions: a case study in the Ejina basin, northwest China. *Environmental Earth Sciences* **75**, 295.

Li, Z., Wang, N., Cheng, H., Li, Y., 2016b. Early–middle Holocene hydroclimate changes in the Asian monsoon margin of northwest China inferred from Huahai terminal lake records. *Journal of Paleolimnology* **55**, 289–302.

Li, Z., Wang, N., Cheng, H., Ning, K., Zhao, L., Li, R., 2015a. Formation and environmental significance of late Quaternary calcareous root tubes in the deserts of the Alashan Plateau, northwest China. *Quaternary International* **372**, 167–174.

Li, Z., Wang, N., Li, R., Ning, K., Cheng, H., Zhao, L., 2015b. Indication of millennial-scale moisture changes by the temporal distribution of Holocene calcareous root tubes in the deserts of the Alashan Plateau, northwest China. *Palaeogeography, Palaeoclimatology, Palaeoecology* **440**, 496–505.

Li, Z., Wei, M., Zhou, J., Tian, X., 2020a. Arid–humid variations in the summer climate and their influence mechanism in Asian monsoon margin of northwest China during 1960–2010: a case study in the Alashan Plateau. *International Journal of Climatology* **40**, 6574–6586.

Li, Z., Zhu, R., Gao, Y., Chim, C.H., Liao, H., 2020b. Recrystallization of Holocene calcareous root tubes in the Tengger Desert, northwest China and its effects on the reliability of paleoenvironmental reconstruction results. *Quaternary International* **562**, 85–93.

Long, H., Lai, Z., Wang, N., Li, Y., 2010. Holocene climate variations from Zhuyeze terminal lake records in East Asian monsoon margin in arid northern China. *Quaternary Research* **74**, 46–56.

Lu, H., Miao, X., Zhou, Y., Mason, J., Swinehart, J., Zhang, J., Zhou, L., Yi, S., 2005. Late Quaternary aeolian activity in the Mu Us and Otindag dune fields (north China) and lagged response to insolation forcing. *Geophysical Research Letters* **32**, L21716.

Lu, H., Wu, N., Liu, K., Jiang, H., Liu, T., 2007. Phytoliths as quantitative indicators for the reconstruction of past environmental conditions in China II: palaeoenvironmental reconstruction in the Loess Plateau. *Quaternary Science Reviews* **26**, 759–772.

Lu, H., Wu, N., Yang, X., Jiang, H., Liu, K., Liu, T., 2006. Phytoliths as quantitative indicators for the reconstruction of past environmental conditions in China I: phytolith-based transfer functions. *Quaternary Science Reviews* **25**, 945–959.

Ma, J., Edmunds, W.M., 2006. Groundwater and lake evolution in the Badain Jaran Desert ecosystem, Inner Mongolia. *Hydrogeology Journal* **14**, 1231–1243.

Ma, N., Wang, N., Zhao, L., Zhang, Z., Dong, C., Shen, S., 2014. Observation of mega-dune evaporation after various rain events in the hinterland of Badain Jaran Desert, China. *Chinese Science Bulletin* **59**, 162–170.

Ma, N., Wang, N., Zhu, J., Chen, X., Chen, H., Dong, C., 2011. Climate change around the Badain Jaran Desert in recent 50 years. [In Chinese with English abstract.] *Journal of Desert Research* **31**, 1541–1547.

McDonald, J., Drysdale, R., Hill, D., 2004. The 2002–2003 El Nino recorded in Australian cave drip waters: implications for reconstructing rainfall histories using stalagmites. *Geophysical Research Letters* **31**, L22202. https://doi.org/10.1029/2004GL020859.

Melnick, D., Garcin, Y., Quinteros, J., Strecker, M.R., Olago, D., Tiercelin, J.-J., 2012. Steady rifting in northern Kenya inferred from deformed Holocene lake shorelines of the Suguta and Turkana basins. *Earth and Planetary Science Letters* **331–332**, 335–346.

Ning, K., Wang, N., Lv, X., Li, Z., Sun, J., An, R., Zhang, L., 2019. A grain size and n-alkanes record of Holocene environmental evolution from a groundwater recharge lake in Badain Jaran Desert, northwestern China. *The Holocene* **29**, 1045–1058.

Peltier, W., 2004. Global glacial isostasy and the surface of the ice-age Earth: the ICE-5 G (VM2) model and GRACE. *Annual Review of Earth and Planetary Sciences* **20**, 111–149.

Piperno, D.R., 2006. *Phytoliths: A Comprehensive Guide for Archaeologists and Paleogeologists*. Altamira Press, New York.

Prebble, M., Schallenberg, M., Carter, J., Shulmeister, J., 2002. An analysis of phytolith assemblages for the quantitative reconstruction of late Quaternary environments of the Lower Taieri Plain, Otago, South Island, New Zealand I. Modern assemblages and transfer functions. *Journal of Paleolimnology* **27**, 393–413.

Pustovoytov, K., Schmidt, K., Parzinger, H., 2007. Radiocarbon dating of thin pedogenic carbonate laminae from Holocene archaeological sites. *The Holocene* **17**, 835–843.

Reimer, P.J., Austin, W., Bard, E., Bayliss, A., Talamo, S., 2020. The IntCal20 Northern Hemisphere radiocarbon age calibration curve (0–55 kcal BP). *Radiocarbon* **62**, 725–757.

Shao, T., Zhao, J., Zhou, Q., Dong, Z., Ma, Y., 2012. Recharge sources and chemical composition types of groundwater and lake in the Badain Jaran Desert, northwestern China. *Journal of Geographical Sciences* **22**, 479–496.

Shen, J., 2013. Spatiotemporal variations of Chinese lakes and their driving mechanisms since the last glacial maximum: A review and synthesis of lacustrine sediment archives. *Chinese Science Bulletin* **58**, 17–31.

Strömberg, C.A.E., 2004. Using phytolith assemblages to reconstruct the origin and spread of grass-dominated habitats in the great plains of North America during the late Eocene to early Miocene. *Palaeogeography, Palaeoclimatology, Palaeoecology* **207**, 239–275.

Sun, J., Hu, W., Wang, N., Zhao, L., An, R., Ning, K., Zhang, X., 2018. Eddy covariance measurements of water vapor and energy flux over a lake in the Badain Jaran Desert, China. *Journal of Arid Land* **10**, 517–533.

Sun, Q., Huguet, A., Zamanian, K., 2021. Outcrop distribution and formation of carbonate rhizoliths in Badain Jaran Desert, NW China. *Catena* **197**, 104975.

ter Braak, C.J.F., Juggins, S., 1993. Weighted averaging partial least squares regression (WA-PLS): an improved method for reconstructing environmental variables from species assemblages. *Hydrobiologia* **269**, 485–502.

Tierney, J.E., Poulsen, C.J., Montanez, I.P., Bhattacharya, T., Feng, R., Ford, H.L., Honisch, B., *et al.*, 2020. Past climates inform our future. *Science* **370**, 6517.

Twiss, P., Suess, E., Smith, R., 1969. Morphological Classification of grass phytoliths. *Soil Science Society of America Journal* **33**, 109–115.

Wang, H., Cheng, Y., Luo, Y., Zhang, C.n., Deng, L., Yang, X., Liu, H., 2019. Variations in erosion intensity and soil maturity as revealed by mineral magnetism of sediments from an alpine lake in monsoon-dominated central east China and their implications for environmental changes over the past 5500 years. *The Holocene* **29**, 1835–1855.

Wang, H., Liu, H., Zhao, F., Yin, Y., Zhu, J., Snowball, I., 2012. Early- and mid-Holocene palaeoenvironments as revealed by mineral magnetic,

https://doi.org/10.1017/qua.2022.31 Published online by Cambridge University Press

geochemical and palynological data of sediments from Bai Nuur and Ulan Nuur, southeastern inner Mongolia Plateau, China. *Quaternary International* **250**, 100–118.

Wang, M., Dong, Z., Luo, W., Lu, J., Li, J., 2015. Spatial variability of vegetation characteristics, soil properties and their relationships in and around China's Badain Jaran Desert. *Environmental Earth Sciences* **74**, 6847–6858.

Wang, N., Ning, K., Li, Z., Wang, Y., Jia, P., Ma, L., 2016. Holocene high lake-levels and pan-lake period on Badain Jaran Desert. *Science China Earth Sciences* **59**, 1633–1641.

Wang, S., Ji, L., 1995. *Paleolimnology of Hulun Lake*. University of Science and Technology of China Press, Hefei.

Wang, W., Liu, J., Zhou, X., 2003. Climate indexes of phytoliths from *Homo erectus*' cave deposits in Nanjing. *Chinese Science Bulletin* **48**, 2005–2009.

Wang, Y., Cheng, H., Edwards, R., He, Y., Kong, X., An, Z., Wu, J., Kelly, M., Dykoski, C., Li, X., 2005. The Holocene Asian monsoon: links to solar changes and North Atlantic climate. *Science* **308**, 854–857.

Wang, Y., Lu, H., 1993. *The Study of Phytolith and Its Application*. China Ocean Press, Beijing.

Webb, E.A., Longstaffe, F.J., 2000. The oxygen isotopic compositions of silica phytoliths and plant water in grasses: implications for the study of paleoclimate. *Geochimica et Cosmochimica Acta* **64**, 767–780.

Wen, R., Xiao, J., Fan, J., Zhang, S., Yamagata, H., 2017. Pollen evidence for a mid-Holocene East Asian summer monsoon maximum in northern China. *Quaternary Science Reviews* **176**, 29–35.

Wünnemann, B., Wagner, J., Zhang, Y., Yan, D., Wang, R., Shen, Y., Fang, X., Zhang, J., 2012. Implications of diverse sedimentation patterns in Hala Lake, Qinghai Province, China for reconstructing Late Quaternary climate. *Journal of Paleolimnology* **48**, 725–749.

Wu, Y., Wang, N., Zhao, L., Zhang, Z., Chen, L., Lu, Y., Lü, X., Chang, J., 2014. Hydrochemical characteristics and recharge sources of Lake Nuoertu in the Badain Jaran Desert. *Chinese Science Bulletin* **59**, 886–895.

Xu, M., Li, Z., 2016. Accumulated temperature changes in desert region and surrounding area during 1960–2013: a case study in the Alxa Plateau, northwest China. *Environmental Earth Sciences* **75**, 1276.

Yang, X., 2000. Landscape evolution and precipitation changes in the Badain Jaran Desert during the last 30 000 years. *Chinese Science Bulletin* **45**, 1042–1047.

Yang, X., Liu, T., Xiao, H., 2003. Evolution of megadunes and lakes in the Badain Jaran Desert, Inner Mongolia, China during the last 31,000 years. *Quaternary International* **104**, 99–112.

Yang, X., Ma, N., Dong, J., Zhu, B., Xu, B., Ma, Z., Liu, J., 2010. Recharge to the inter-dune lakes and Holocene climatic changes in the Badain Jaran Desert, western China. *Quaternary Research* **73**, 10–19.

Yang, X., Scuderi, L.A., 2010. Hydrological and climatic changes in deserts of China since the late Pleistocene. *Quaternary Research* **73**, 1–9.

Yang, X., Scuderi, L., Paillou, P., Liu, Z., Li, H., Ren, X., 2011. Quaternary environmental changes in the drylands of China—a critical review. *Quaternary Science Reviews* **30**, 3219–3233.

Yang, X., Williams, M.A.J., 2003. The ion chemistry of lakes and late Holocene desiccation in the Badain Jaran Desert, Inner Mongolia, China. *Catena* **51**, 45–60.

Yi, L., Lu, X., Nie, Z., Wang, H., Cheng, K., Yang, Y., Li, L., 2020. Delineation of groundwater flow and estimation of lake water flushing time using radium isotopes and geochemistry in an arid desert: the case of Badain Jaran Desert in western Inner Mongolia (CHN). *Applied Geochemistry* **122**, 104740.

Zamanian, K., Pustovoytov, K., Kuzyakov, Y., 2016. Pedogenic carbonates: forms and formation processes. *Earth-Science Reviews* **157**, 1–17.

Zhang, H., Peng, J., Ma, Y., Chen, G., Feng, Z., Li, B., Fan, H., Chang, F., Lei, G., Wünnemann, B., 2004. Late Quaternary palaeolake levels in Tengger Desert, NW China. *Palaeogeography, Palaeoclimatology, Palaeoecology* **211**, 45–58.

Zhao, J., Li, X., 2018. Spatial complexity of lake water ions in the Badain Jaran Desert. *Journal of Lake Sciences* **30**, 680–692.

Zhu, J., Wang, N., Chen, H., Dong, C., Zhang, H., 2010. Study on the boundary and the area of Badain Jaran Desert based on remote sensing imagery. [In Chinese with English abstract.] *Progress in Geography* **29**, 1087–1094.

Zhu, R., Li, Z., Gao, Y., Chen, Q., Yu, Q., 2019. Variations in chemical element compositions in different types of Holocene calcareous root tubes in the Tengger Desert, NW China, and their palaeoenvironmental significance. *Boreas* **48**, 800–809.

Zuo, X., Lu, H., Li, Z., Song, B., 2021. Phytolith reconstruction of early to mid-Holocene vegetation and climatic changes in the Lower Yangtze Valley. *Catena* **207**, 105586.

Zuo, X., Lu, H., Li, Z., Song, B., Xu, D., Zou, Y., Wang, C., Huan, X., He, K., 2016. Phytolith and diatom evidence for rice exploitation and environmental changes during the early mid-Holocene in the Yangtze Delta. *Quaternary Research* **86**, 304–315.

https://doi.org/10.1017/qua.2022.31 Published online by Cambridge University Press